Thermographic investigation of the effect of plasma exposure on the surface of a MAST upgrade divertor tile in Magnum-PSI

M.J. Dunn [a,b,*], T.W. Morgan [c], J.W. Genuit [c], T. Loewenhoff [d], A.J. Thornton [b], K.J. Gibson [a], the Magnum-PSI team [c]

[a] *York Plasma Institute, Department of Physics, University of York, Heslington, York, YO10 5DD, United Kingdom*
[b] *United Kingdom Atomic Energy Authority, Culham Science Centre, Abingdon, Oxfordshire, OX14 3DB, United Kingdom*
[c] *DIFFER - Dutch Institute for Fundamental Energy Research, De Zaale 20, 5612 AJ Eindhoven, The Netherlands*
[d] *Forschungszentrum Jülich, Institut für Energie und Klimaforschung, 52428 Jülich, Germany*

ARTICLE INFO

ABSTRACT

One of the issues faced by future fusion devices will be high divertor target heat loads. Alternative divertors can promote detachment, flux expansion and dissipation mechanisms to mitigate these heat loads. They have been investigated in several devices including TCV and DIII-D, and will be investigated on MAST-U. To evaluate their effectiveness, accurate target heat flux and power balance measurements are required in these machines. Infrared (IR) thermography is a widely used technique to determine the target heat flux, but is susceptible to surface effects and emissivity in carbon-walled machines. In this work, the effect of plasma exposure on graphite is assessed to understand what may happen in MAST-U. A sample of fine grain graphite, as used on MAST-U, is exposed to 30 min plasma exposures, with density $n_e = 6 \times 10^{18}\,\mathrm{m^{-3}}$ and temperature $T_e = 0.08\,\mathrm{eV}$ as measured by Thomson scattering. During these pulses, the temperature is measured by a medium wave IR camera and is seen to decrease by $\approx$70 °C over the course of 3 h of plasma exposure. Pyrometer measurements suggest that the IR camera data is affected by a change in the surface emissivity. Profilometry confirms erosion of graphite at the tile centre to a depth of $\approx$100 μm, and a larger region of deposition further out, amounting to $\approx$40 μm of material.

1. Introduction

The problem of handling the extreme heat and particle fluxes to plasma facing components is one of the major challenges facing the design of the next generation of fusion devices. The heat loads associated with ITER [1] and DEMO [2,3] like devices are at or above the limit of thermal performance of existing materials and, as a result, alternative approaches to divertor geometries are being investigated on devices such as MAST-U [4].

To characterise the performance of different divertor geometries requires a careful accounting of the various power sources and sinks in the tokamak, necessitating the use of many different diagnostic techniques. In particular, the direct measurement of divertor heat load is challenging and is usually obtained either through electrostatic probes, thermocouples, infrared (IR) thermography, or a combination thereof. The last of these approaches is susceptible to interference from surface effects and changes in emissivity, since changes to the surface properties of plasma facing components such as divertor tiles can lead to significant changes to the inferred temperature of the tile surface (and hence the calculated heat flux onto the tile). This is especially true in tokamaks with carbon walls, such as MAST-U.

For this reason, it is important to understand the impact of plasma–surface interactions on the tile surface, and also to monitor how these can affect IR measurements over extended periods of plasma operation. To perform such a systematic study on an actual tokamak device is challenging since the divertor tile surfaces typically evolve over a time period representing many thousands of tokamak pulses, encompassing many different operating scenarios and imposed heat loads.

To address this, in these studies we present initial results from the systematic exposure of a divertor tile from MAST-U on the Magnum-PSI linear plasma device. These experiments have sought to identify changes in the tile surface properties over a period of many hours of reproducible plasma operation, and how these can lead to significant changes in the observed heat fluxes inferred from IR measurements.

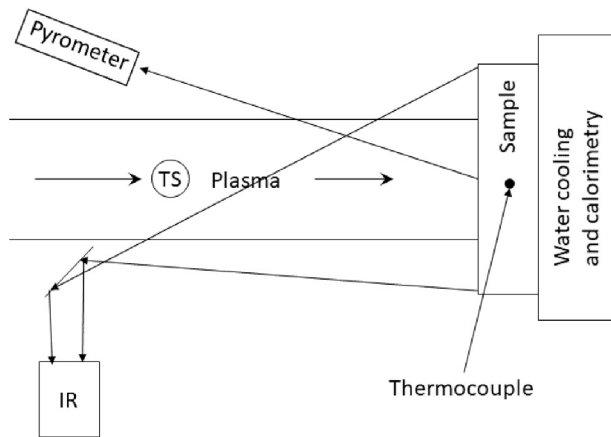**Fig. 1.** A diagram of the experimental setup, showing the position of key diagnostics (dimensions not to scale).
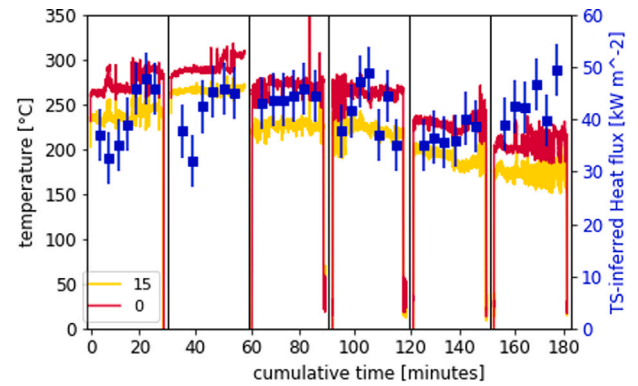

Fig. 2. The temperature of certain regions of the tile as measured by the IR camera (labelled by distance from the centre in mm) throughout the long pulses. On the second axis, the heat flux inferred from Thomson scattering, using a similar method to [6] (blue squares) with error estimated from the instrument resolution.

2. Experimental method

The tile used was a fine grain graphite tile, identical to those that will be used in the MAST-U divertor. The sample measured approximately 150×150×15 mm. The Magnum-PSI linear plasma device (located at the Dutch Institute For Fundamental Energy Research — DIFFER) can deliver a continuous plasma of ≈ 2 cm beam radius (FWHM) to the tile surface for extended periods (several hours if desired), allowing a plasma exposure equivalent to a MAST-U campaign in a single day.

In order to maintain a tile surface temperature comparable to that expected in MAST-U, Magnum-PSI was operated with a magnetic field of 0.5 T, current of 140 A and hydrogen gas flow of 10 standard litres per minute (slm) with 1.5 slm gas puffing near the target. This resulted in plasma electron density of $5 - 7 \times 10^{18}$ m^{-3} and electron temperature of $0.07 - 0.09$ eV as measured by Thomson Scattering (TS). Numerous other diagnostics were also used, including a FLIR SC7500M infrared camera (filtered at 4 μm), and a FAR SpectroPyrometer FMPI, operating at $900 - 1700$ nm (enabling an emissivity-independent temperature measurement). There was also an in-tile thermocouple, located in a hole drilled into the side of the tile to the centre, and a calorimetry system, giving an indication of heat conducted out of the active water cooling system at the back of the tile.

The basic experimental setup for these experiments is shown in Fig. 1. The TS measurement was taken 81.5 mm from the sample surface in the centre of the plasma column. An indication is also given as to the arrangement of the IR camera and the pyrometer, but the dimensions are not to scale; the viewing angles are approximately 30° from the surface normal.

The tile was exposed to plasma for six 30-minute intervals, with the parameters above including 1.5 slm gas puffing. These 30-minute plasma exposures were continuously monitored by the IR camera at 25 Hz. There were TS measurements at five-minute intervals, each of which was averaged over 100 measurements to minimise the statistical uncertainty of the measurement at such low temperatures and densities.

In order to allow additional temperature measurements with a multiwavelength pyrometer (which operates only at temperatures above 550 °C), the tiles were exposed to higher plasma power for 1 min intervals, in between the longer plasma exposures mentioned above. Because it measures at multiple wavelengths, the pyrometer gives a measurement that is independent of the tile emissivity, assuming the emissivity does not vary within the $900 - 1700$ nm wavelength range. This technique can even be used to measure the emissivity [5]. The higher plasma power to the tiles was achieved by lowering the target gas puffing from 1.5 to 0.5 slm, resulting in plasma conditions of $n_e \approx 2 \times 10^{19}$ m^{-3} and $T_e \approx 0.15$ eV.

After these experiments had taken place, the tile was sent to Forschungszentrum Jülich, for a surface topology profile to be taken using a laser profilometer with a KF3 sensor from OPM Messtechnik GmbH. This offers insight into whether the observations from the experiments were caused by erosion or deposition (or a combination thereof). The profilometer also reports surface reflectivity, at a wavelength of 670 nm which can be used to validate any conclusions about changes to the tile emissivity. After this, the tile was returned to Culham and viewed at room temperature using an infrared camera.

3. Results

Fig. 2 shows the temperature evolution of the tile when it was exposed repeatedly to 30-minute plasma discharges. The temperature at the centre of the beam and at a location 15 mm from the centre of the beam are shown as a function of the plasma exposure time, assuming an emissivity of 0.65. It can be seen that the apparent temperature decreased by about 70 °C during this time. The trend is approximately linear, suggesting that it was not approaching a saturation point, but would have continued to decrease for several more hours. Temperature measurements from the thermocouple are not shown, because the thermocouple was several millimetres below the surface of the tile, and only registered a temperature 1 °C above room temperature during the long pulses, except during the fifth pulse, when it recorded a 2 °C increase. The heat flux to the tile has been estimated using the temperature and density measurements from the Thomson scattering measurements, and was approximately constant throughout.

The results of the short exposures are shown in Fig. 3. Similar to the long exposures, the infrared camera reports a decrease in surface temperature during (and in some cases between) these shorter pulses, of about 140 °C. The heat flux derived from TS data, although it suffers from random noise, had no discernible downward trend. Temperature readings from the pyrometer were available for the short pulses because of the higher temperatures, and are directly comparable with the IR reading of the centre of the plasma. This suggests that the temperature was not actually decreasing. The thermocouple recorded a temperature increase of $(6 \pm 1)°$ C during the short pulses. If the temperature were in fact decreasing as suggested by the IR, a 1 °C drop would be expected on the thermocouple, however this is within the measurement error. As such, the thermocouple data was not factored into our conclusions. The agreement between IR and pyrometer in the fifth exposure suggests that the emissivity was equal to the assumed value of 0.65 at this time (after 2.5 h of exposure).

In both Figs. 2 and 3 the heat flux is calculated using appropriate temperature-dependent values of sheath heat transmission coefficient. These values are unusually high, in the region of $\gamma \approx 100 - 200$,
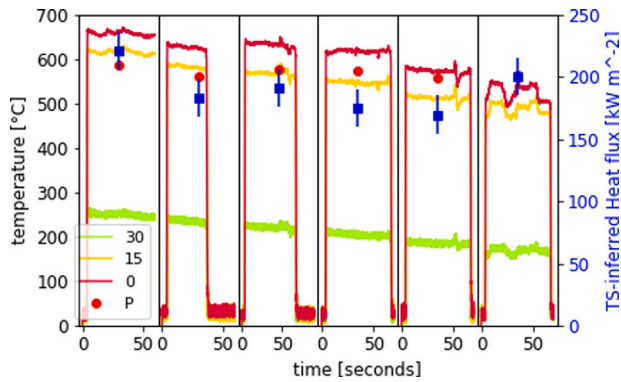
Fig. 3. The temperature of certain regions of the tile as measured by the IR camera (labelled by distance from the centre in mm), and also the temperature measured by the multi-wavelength pyrometer (red dots labelled P). On the second axis, the heat flux inferred from Thomson scattering, using a similar method to [6] (blue squares) with error estimated from the instrument resolution.

Fig. 4. Photograph of the tile surface after the experiments, with lighter and darker rings visible. The red box indicates the portion of the tile shown in Figs. 5 and 6.

Fig. 5. The surface reflectivity of part of the tile that was exposed to the plasma (indicated by the red box in Fig. 4. The measurement was made at 670 nm.

Fig. 6. The surface profile of part of the tile that was exposed to the plasma (indicated by the red box in Fig. 4. Profile (z) resolution is 20 nm averaged over 1 unit of the lateral (x and y) resolution, which is 10 μm.

because the non-linear inverse temperature dependence of γ becomes significant at such low temperatures [7]. Two dimensional modelling of the tile temperature evolution shows that this calculated heat flux is too low to reproduce the observed temperature rise of the tile. A simple finite-element model was used, simulating only the first 450 ms of each pulse, which is the time taken for the heat to conduct to the back of the tile, since the model does not account for active cooling. Note that this time is much shorter than the time the tile would take to reach thermal equilibrium. To match the temperature rise seen in the experiment, the required heat flux is of the order $2 \, \text{MW} \, \text{m}^{-2}$ for the 30-minute exposures and $7 \, \text{MW} \, \text{m}^{-2}$ for the 1-minute exposures. These calculated values are comparable to the machine input power. However, it is conceivable that the normal method for calculating γ no longer applies at temperatures $< 0.1 \, \text{eV}$. The determination of an appropriate value of γ is the subject of ongoing study.

In both experiments, the IR-inferred temperature of the tile was found to decrease during and between plasma exposures, despite the heat flux (inferred from either TS or machine power) remaining constant. Investigation of the rate of cooling at the end of each exposure shows no evidence of the sudden cooling associated with a surface layer [8]. The pyrometer in the short exposures showed no decrease in temperature. Such an inferred decrease in temperature could be explained by a change in tile surface emissivity.

3.1. Post mortem analysis

After the experiments had taken place, visible inspection of the tile showed rings of alternating lightening and darkening, as seen in Fig. 4. These rings are circular, centred around where the plasma was incident on the tile (except the thin outer ring, which is an artefact of the Magnum-PSI skimmer). The rings are also visible in surface visible light reflectivity measurements, see Fig. 5. The higher reflectivity measured in the centre of the tile corresponds to the lower emissivity observed in the experiment. A topology profile, given in Fig. 6, shows that this equates to erosion and deposition. Erosion causes the surface emissivity to lower (it appears lighter) and erosion of up to 100 μm is observed within the FWHM of the plasma column. At such low plasma temperatures and densities, this is likely due to chemical erosion rather than physical sputtering. At the periphery of the plasma, where the plasma power was lower, similar to the MAST divertor, the plasma–surface interactions were deposition dominated, with deposits up to 40 μm thick. This caused the surface to become darker, thereby raising the emissivity in this region.

This has been observed before on MAST, as shown in Fig. 7. It can be seen that the recently replaced tile in the centre of the figure has a
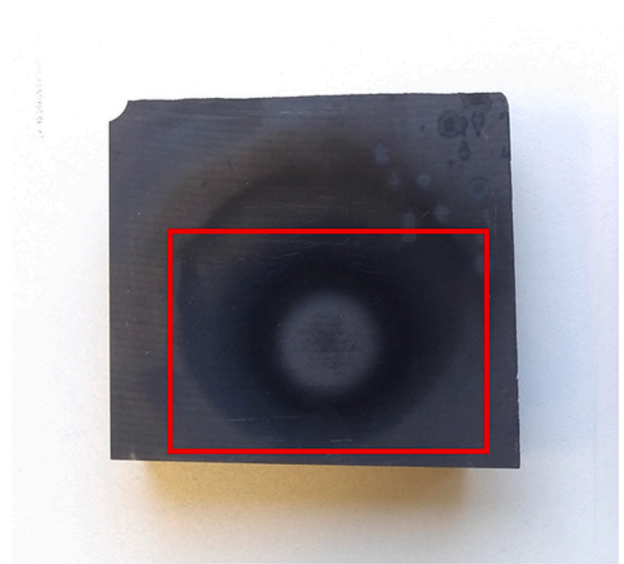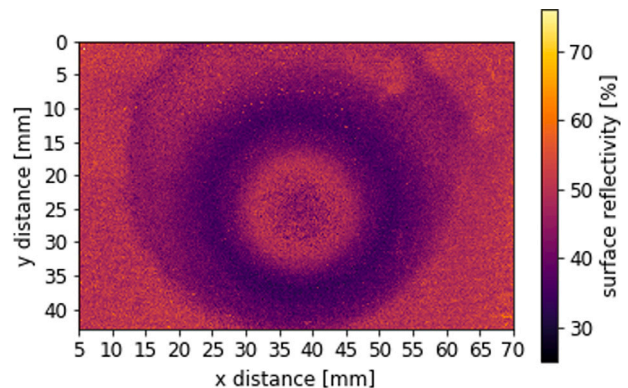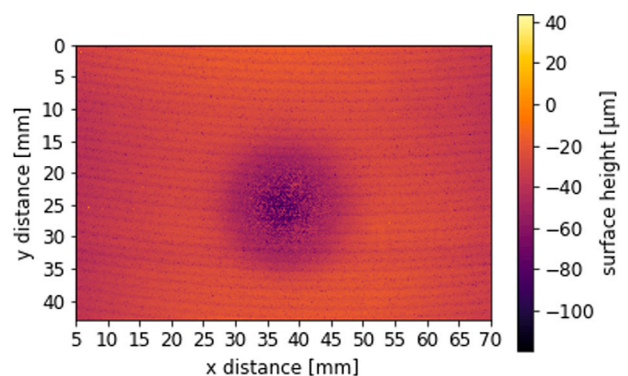
lower emissivity than the others. This is because those other tiles had slowly increased in emissivity during exposure to low power plasma, as happened around the periphery of the tile used in this experiment. The same effect has also been observed on ASDEX Upgrade [9].

Fig. 7. Some of the tiles in the divertor of MAST during shot 25 735. The tile in the centre of the image had just been replaced, and the strike point is very faint on this tile compared to the others.
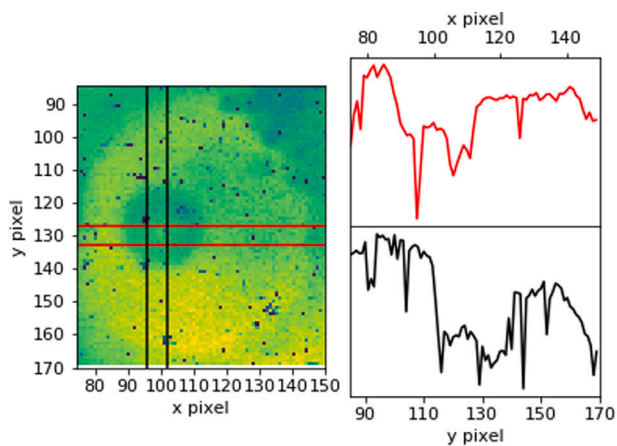

Fig. 8. An infrared image of the tile at room temperature, with no heat applied, showing the contrast caused by the varying emissivity. Left is the full image, right are horizontal and vertical line profiles, each averaged over the 7 highlighted rows of pixels, shown in red and black respectively. (For interpretation of the references to colour in this figure legend, the reader is referred to the web version of this article.)

After the tile was brought back to Culham, an image of the tile at room temperature was taken using a long wave infrared camera. This image is shown in Fig. 8a. The contrast in this image, the small darker circle off-centre within the lighter circle, corresponds to the same circles visible in Figs. 4 and 5. Because no heat sources were being applied to the tile when Fig. 8 was taken, the inferred temperature gradient across the surface can only have been caused by a spatial variation in emissivity. Looking at a horizontal or vertical slice of this image (Fig. 8b and c respectively) the step caused by the area of lower emissivity can clearly be seen.

4. Conclusion

The results presented in this paper suggest that exposure to certain plasma conditions decreases the surface emissivity of the graphite, which reduced the apparent temperature of the tile over time. This conclusion is supported by an inferred temperature gradient in an image of the unheated tile. Erosion can clearly be seen at the centre of the tile, and therefore no surface layers are deposited there. Further from the centre, there are signs of deposition, similar to what has been observed on the inner divertor of MAST. Further analysis of these experiments will include a focus on these areas of the tile, and what the implications are for MAST-U.

In particular, consideration must then be given to any inaccuracies in the procedure for analysis of MAST-U data which become apparent as a result. This analysis uses a code called THEODOR, and proceeds according to the process described in [10]. It uses a parameter called heat transmission factor, α, which is a single scalar parameter intended to account for a non-uniform temperature distribution near the surface, which could cause a sudden surface temperature jump, and is defined as $\alpha = \lambda_{layer}/d$ where λ_{layer} is the heat conduction coefficient and d is the layer thickness [11]. It does not account for the possibility of erosion lowering the emissivity. This greater understanding may lead to a change in the analysis used for MAST-U.

This investigation does not account for the influence of transient loading on the evolution of MAST-U divertor tiles. To examine this further, a second tile was exposed to ELM-like plasma loading in Magnum-PSI [12]. Initial analysis shows similar emissivity decrease as presented here. Further analysis is ongoing.

CRediT authorship contribution statement

M.J. Dunn: Conceptualisation, Methodology, Investigation, Writing - original draft, Visualisation. **T.W. Morgan:** Methodology, Resources, Writing - review & editing. **J.W. Genuit:** Formal analysis. **T. Loewenhoff:** Investigation, Writing - review & editing. **A.J. Thornton:** Resources, Writing - review & editing, Supervision. **K.J. Gibson:** Conceptualisation, Supervision.

Declaration of competing interest

The authors declare that they have no known competing financial interests or personal relationships that could have appeared to influence the work reported in this paper.

References

[1] K. Ikeda, Progress in the ITER physics basis, Nucl. Fusion 47 (6) (2007) URL http://stacks.iop.org/0029-5515/47/i=6/a=E01.

[2] R.P. Wenninger, M. Bernert, T. Eich, E. Fable, G. Federici, A. Kallenbach, A. Loarte, C. Lowry, D. McDonald, R. Neu, T. Pütterich, P. Schneider, B. Sieglin, G. Strohmayer, F. Reimold, M. Wischmeier, DEMO divertor limitations during and in between ELMs, Nucl. Fusion 54 (11) (2014) 114003, URL http://stacks.iop.org/0029-5515/54/i=11/a=114003.

[3] N. Asakura, K. Shimizu, K. Hoshino, K. Tobita, S. Tokunaga, T. Takizuka, A simulation study of large power handling in the divertor for a Demo reactor, Nucl. Fusion 53 (12) (2013) 123013, http://dx.doi.org/10.1088/0029-5515/53/12/123013, URL https://iopscience.iop.org/article/10.1088/0029-5515/53/12/123013.

[4] W. Morris, J.R. Harrison, A. Kirk, B. Lipschultz, F. Militello, D. Moulton, N.R. Walkden, MAST upgrade divertor facility: A test bed for novel divertor solutions, IEEE Trans. Plasma Sci. 46 (5) (2018) 1217–1226.

[5] V. Tank, H. Dietl, Multispectral infrared pyrometer for temperature measurement with automatic correction of the influence of emissivity, Infrared Phys. 30 (4) (1990) 331–342.

[6] T. Morgan, M. van den Berg, G. De Temmerman, S. Bardin, D. Aussems, R. Pitts, Power deposition on misaligned castellated tungsten blocks in the Magnum-PSI and Pilot-PSI linear devices, Nucl. Fusion 57 (12) (2017) 126025, http://dx.doi.org/10.1088/1741-4326/aa8109, URL https://iopscience.iop.org/article/10.1088/1741-4326/aa8109.

[7] M.A. Van Den Berg, K. Bystrov, R. Pasquet, J.J. Zielinski, G. De Temmerman, Thermographic determination of the sheath heat transmission coefficient in a high density plasma, J. Nucl. Mater. 438 (Suppl) (2013) http://dx.doi.org/10.1016/j.jnucmat.2013.01.087.

[8] F. Lott, A. Kirk, G.F. Counsell, J. Dowling, D. Taylor, T. Eich, A. Herrmann, Thermographic power accounting in MAST, J. Nucl. Mater. (2005) http://dx.doi.org/10.1016/j.jnucmat.2004.10.053.

[9] A. Herrmann, B. Sieglin, M. Faitsch, Surface temperature measurement of in-vessel components and its real-time validation, Fusion Sci. Technol. 69 (3) (2016) 569–579, http://dx.doi.org/10.13182/FST15-187.

[10] A. Herrmann, W. Junker, K. Gunther, S. Bosch, M. Kaufmann, J. Neuhauser, G. Pautasso, T. Richter, R. Schneider, Energy flux to the ASDEX-upgrade diverter plates determined by thermography and calorimetry, Plasma Phys. Control. Fusion 37 (1) (1995) 17–29, http://dx.doi.org/10.1088/0741-3335/37/1/002, URL https://iopscience.iop.org/article/10.1088/0741-3335/37/1/002.

[11] A. Herrmann, A.U. Team, Limitations for divertor heat flux calculations of fast events in Tokamaks, in: C. Silva, C. Varandas, D. Campbell (Eds.), 28th EPS Conference on Controlled Fusion and Plasma Physics. Contributed Paper, in: ECA, vol. 25A, European Physical Society, Funchal, 2001, pp. 2109–2112.

[12] T.W. Morgan, T.M. de Kruif, H.J. van der Meiden, M.A. van den Berg, J. Scholten, W. Melissen, B.J.M. Krijger, S. Bardin, G. De Temmerman, A high-repetition rate edge localised mode replication system for the magnum-PSI and Pilot-PSI linear devices, Plasma Phys. Control. Fusion 56 (9) (2014) 095004, http://dx.doi.org/10.1088/0741-3335/56/9/095004, URL http://stacks.iop.org/0741-3335/56/i=9/a=095004?key=crossref.13871096e1e8be4ed77490031be37c8d.